

Photochemical Reactions in the Interior of a Zeolite. Part 5: The Origin of the Zeolite Induced Regioselectivity in the Singlet Oxygen Ene Reaction

Edward L. Clennan* and Jakub P. Sram

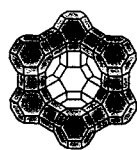
Department of Chemistry, University of Wyoming, Laramie, WY 82071 USA

Received 25 February 2000; revised 15 March 2000; accepted 17 March 2000

Abstract—Photooxidations of several new alkenes in the interior of methylene blue doped NaY are reported. The results suggest that the novel regiochemistry of these reactions can be rationalized by invoking both cation complexation with the alkenes and electrostatic interaction between the cation and the pendant oxygen on the developing perepoxide. © 2000 Elsevier Science Ltd. All rights reserved.

Introduction¹

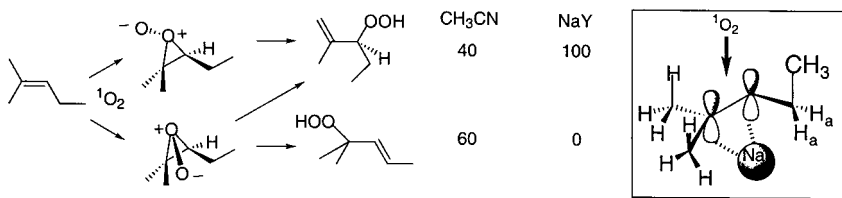
Supramolecular control of photochemical reactions provides a powerful tool to control and alter photochemical behavior.^{2,3} Zeolites, in particular are attractive hosts because of their well-characterized structures and properties.^{4,5} Faujasites NaY and NaX (Scheme 1) have attracted considerable attention because of their availability and pore structure which can easily accommodate organic molecules of interest to the organic chemist. NaY and NaX have the same topographical structure and only differ in their Si/Al ratio. These crystalline porous aluminosilicate solids consist of silicon and aluminum tetrahedra connected by bridging



Faujasite

vertices - silicon or aluminum atoms
— oxygen bridges

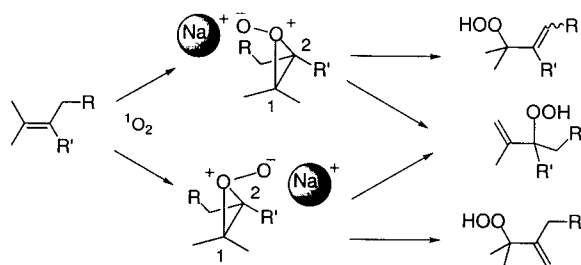
Scheme 1.



Scheme 2.

Keywords: zeolites; singlet oxygen; photooxidation; ene reaction; allylic hydroperoxides; sensitizers.

* Corresponding author. Tel.: +1-307-766-6667; fax: +1-307-766-2807; e-mail: clennane@uwyo.edu



Scheme 3.

end of the double bond. (Scheme 2) This dramatically enhanced regioselectivity was tentatively attributed to complexation of the olefin to a Na^+ compelling the sterically demanding allylic methyl group to rotate to the face approached by $^1\text{O}_2$, thereby preventing access to the allylic hydrogens H_a on the methylene carbon. (Scheme 2)

Clennan and Sram^{1b} examined the photooxidations of a series of tetra-substituted alkenes in MB doped NaY and suggested that cation complexation to the pendant oxygen in the perepoxide intermediate was the regiochemical important interaction. (Scheme 3) This model suggested that Markovnikov directing effects, as a result of greater charge buildup on the carbon framework, and the preferential formation of the perepoxide with the pendant oxygen on the least substituted *side* of the double bond, were responsible for the observed regiochemistry.

We report here new results with trisubstituted alkenes that demonstrate that both cation complexation to the alkene, and the electrostatic interaction of the cation with the pendant oxygen, are important in determining the regiochemistry of the intrazeolite photooxidation. We also report that as a result of the electrostatic stabilization of the perepoxide the '*cis*-effect' which operates in solution is diminished in importance in the intrazeolite photooxidations.

Results and Discussion

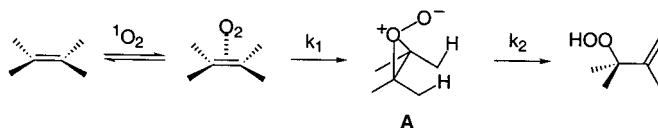
Preparation of NaMBY

MB doped NaY was synthesized by using a procedure similar to that reported by Ramamurthy and coworkers.⁶ A weighed sample of NaY was added to an aqueous solution of MB and allowed to stir until the blue solution turned colorless. The MB doped NaY (NaMBY) was then filtered and air dried followed by additional drying on a vacuum line at 10^{-4} Torr and $100\text{--}120^\circ\text{C}$ for 8–10 h. It was then removed from the vacuum line and stored in a desiccator prior to use. When the doped zeolite is used directly off the vacuum line for photooxidations of 2,3-dimethyl-2-butene,

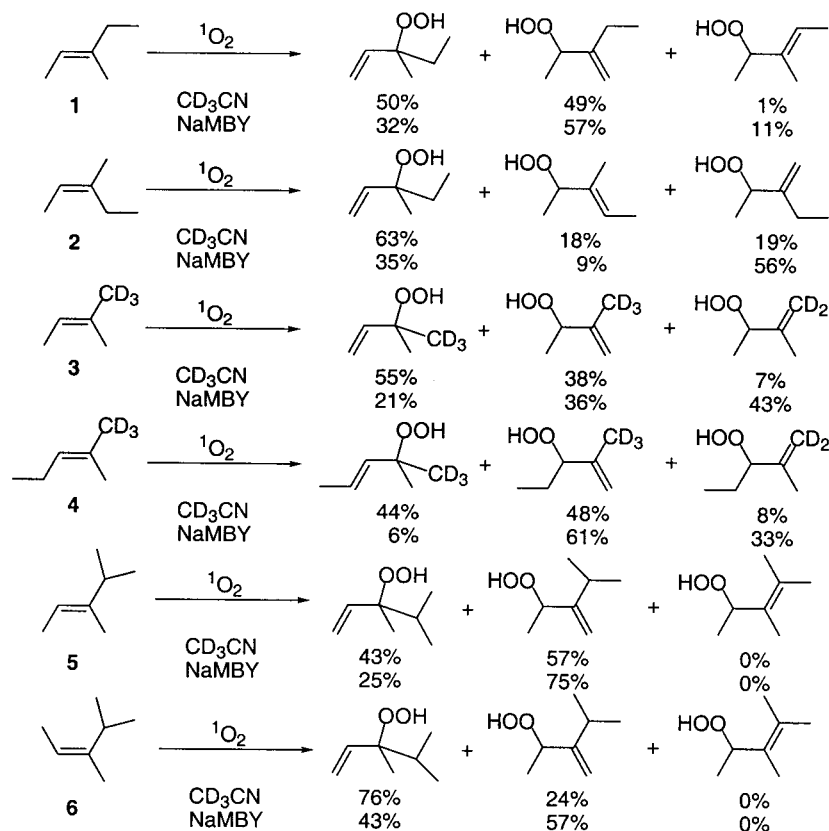
and 2-methyl-2-pentene, in addition to the anticipated allylic hydroperoxides, small amounts of the corresponding reduced species, the allylic alcohols were also observed. Addition of triphenyl phosphine to the reaction mixtures converted the remaining allylic hydroperoxides to these same allylic alcohols. In contrast, the use of NaMBY stored for extended periods of time, that presumably absorbed some atmospheric water, did not produce any alcohol byproducts which highlights the importance of water in these reactions.

Photooxidations of trisubstituted alkenes **1–6** were conducted using 0.012 to 0.018 M alkene in 5 mL of hexane, a photolysis time of 10 min., a 550 nm solution cutoff filter, a $\langle S \rangle_{\text{MB}} = 0.0001$ (number of MB molecules per supercage), and samples of NaMBY which had been stored in a desiccator after drying on the vacuum line.¹⁰ These conditions were chosen in order to minimize any possible allylic hydroperoxide decomposition which might mask the true reaction regioselectivity.¹¹ Trisubstituted alkenes **1–6** were chosen for examination in order to determine the effect of the zeolite environment on both side and end selectivity of the ene reaction. All the alkenes were also photooxidized in CD_3CN to provide a direct comparison to the reactions in the interior of the zeolite. A stepwise mechanism that is supported by a considerable amount of experimental data has previously been established in homogenous solution¹² (Scheme 4) and a key intermediate, the perepoxide **A**, has also been implicated in intrazeolite photooxidations.¹³

Examination of the regiochemistry in CD_3CN reveals that the hydrogen abstraction occurs overwhelmingly from the most hindered side of the alkene. (99% in **1**; 81% in **2**; 93% in **3**; and 92% in **4**) This phenomenon, which has previously been observed, has become known as the '*cis* effect' and was first recognized in enol ethers by Conia¹⁴ and Foote.¹⁵ This propensity to abstract hydrogen on the most congested side of the alkene was also observed in acyclic¹⁶ and cyclic¹⁷ aliphatic alkenes. Two different models have been suggested to explain the '*cis* effect'. In the Stephenson/Fukui model^{18,19} a favorable HOMO–LUMO interaction between the trailing oxygen in the incipient perepoxide and the allylic hydrogens is maximized on the more congested side of the olefin. In an interesting suggestion, Houk and coworkers²⁰ suggested that the barrier to rotate the allylic hydrogen to the perpendicular geometry favorable for abstraction plays a dominant role in dictating the regiochemistry of the reactions. Their calculations demonstrated that the eclipsed geometry of a methyl group is destabilized and its rotation barrier lowered when buttressed by a *cis* substituent. The Houk model has been criticized and its inability to predict the correct regiochemistry when sterically demanding groups are present has been pointed out.²¹ However, regardless of the origin of the '*cis* effect' it provides a useful tool to engineer the regiochemistries of singlet oxygen ene reactions (Scheme 5).



Scheme 4.



Scheme 5.

The end selectivities in the homogeneous photooxidations are very small ($[(\text{disubstituted end})/(\text{monosubstituted end})]$; **1**, 50/50; **2**, 37/63; **3**, 45/55; **4**, 56/44; **5**, 57/43; and **6**, 24/76) indicative of the absence of a Markovnikov directing effect in these reactions. This suggests that in CD_3CN that there is very little charge on the carbon framework of the peroxide, (**A** in Scheme 4) or that it is the magnitude of the interaction of the pendant oxygen with the allylic hydrogens, rather than the charge on the carbon framework, which dictates the regiochemistry of hydrogen abstraction.

The regiochemistries of the ene reactions are dramatically different in the intrazeolite photooxidations. In particular, the 'cis effect' is significantly diminished. As the photooxidation is moved from CD_3CN to the interior of the zeolite the amount of hydrogen abstraction from the most hindered side of the olefin decreases from 99 to 89% in **1**; from 81 to 44% in **2**; from 93 to 57% in **3**; from 92 to 67% in **4**; and from 76 to 43% in **6**. This change in regioselectivity is consistent with the model depicted in Scheme 3, in which the peroxide with the sodium complexed to the pendant oxygen on the least substituted side alkene is sterically preferred over its diastereomer with the sodium ion on the more congested side of the alkene. Clearly the loss of stabilization provided by the interaction between the pendant oxygen and the allylic hydrogens is more than compensated for by the electrostatic interaction with the sodium cation.

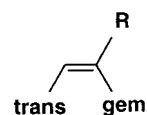
The *gem/trans* ratios in Table 1 are a measure of the end selectivity (Markovnikov directing effect) for the peroxides formed on the most congested side of the olefin. This end selectivity (*gem/trans*) increases from 0.98 to 1.78

in **1**, from 0.69 to 1.71 in **3**, and from 1.33 to 3.0 in **5** as the medium is changed from CD_3CN to NaMBY. Consequently, Markovnikov directing effects are more important in the zeolite than in solution consistent with our earlier suggestion of increased charge on the carbon framework of the peroxide in the zeolite.

The magnitudes of the increases in the Markovnikov directing effects for all trialkyl substituted alkenes should be similar to those observed for **1**, **3**, and **5** (a factor of 1.8 to 2.5) since inductively similar substituents (σ_1 for Me, Et, and *i*Pr are -0.04 , -0.05 , and -0.06 , respectively)²² should support the same charge distribution on the two sp^2 alkene carbons. However, the *gem/trans* ratio in **2** exhibits a small decrease (from 0.29 to 0.26) and the *gem/trans* ratio in **4** exhibits an unexpectedly large increase from 1.09 to 10.2. In both cases, this represents a decreased ability for hydrogen

Table 1. End selectivity on the most congested side of the alkene

Compound	<i>gem/trans</i>	
	CH_3CN	Zeolite
1	0.98	1.78
2	0.29	0.26
3	0.69	1.71
4	1.09	10.2
5	1.33	3.0



abstraction from an ethyl to compete with hydrogen abstraction from a methyl group in the intrazeolite in comparison to the homogeneous photooxidations. It is difficult to explain this behavior within the framework of the model depicted in Scheme 3. The Ramamurthy model (Scheme 2), on the other hand, can explain the *gem/trans* ratio in both **2** and **4**. Rotation of the ethyl group in **2** to place the methyl on the same face of the alkene approached by singlet oxygen, as predicted by the Ramamurthy model, would prevent access to the methylene hydrogens and decrease the end selectivity below that anticipated for the Markovnikov directing effect. The identical effect operating in **4** would diminish hydrogen abstraction on the least substituted end of the alkene and enhance the Markovnikov directing effect consistent with the experimental observation. (Table 1)

The partial success of both the Scheme 3 and Ramamurthy (Scheme 2) models suggest that a composite model might be universally beneficial. We suggest such a composite model in Scheme 6 which recognizes that complexation of sodium to both the alkene and the pendant oxygen in the perepoxide are important aspects of intrazeolite photooxidations. In this model as singlet oxygen approaches the alkene the sodium cation adopts a position which allows a favorable electrostatic interaction with both the pendant oxygen in the perepoxide and the negatively charged aluminum in the zeolite framework. The formation of the perepoxide with the sodium on the least substituted side of the olefin is both kinetically and thermodynamically preferred and as a consequence the 'cis effect' is diminished in intrazeolite singlet oxygen ene reactions. In addition, the proximity of the complex to the wall of the supercage enhances the likelihood of approach of singlet oxygen to the face of the olefin occupied by the allylic substituent R' (Scheme 6).

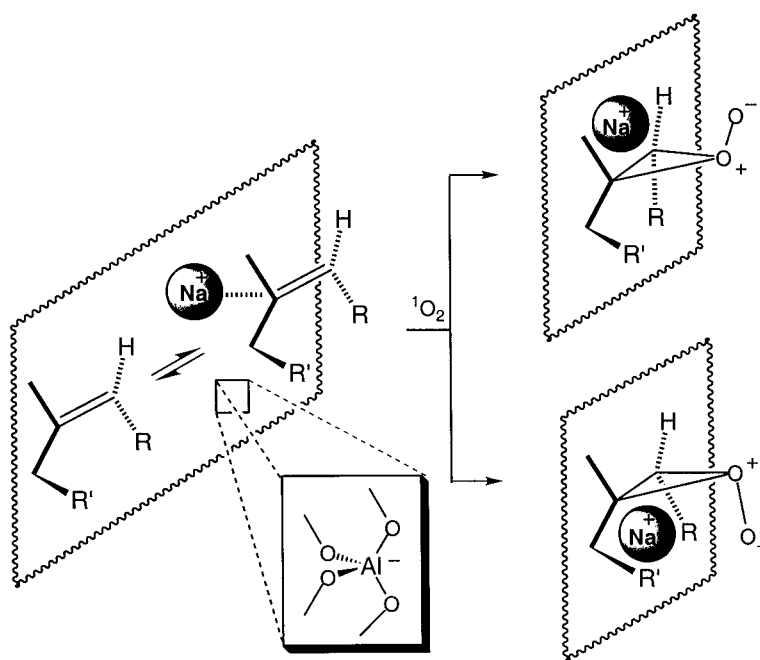
Our results cannot distinguish between addition of singlet oxygen to the cation complexed alkene or to a small amount of free alkene that is in equilibrium (Scheme 6) with the

complex. If found near the zeolite framework, this newly liberated alkene might exhibit the Ramamurthy (Scheme 2) steric effect and still be close enough to the sodium cation to allow electrostatic stabilization of the perepoxide. The free alkene would be expected to be considerably more nucleophilic than the complexed alkene and would react much faster with singlet oxygen. On the other hand, the electronic stabilization of the incipient perepoxide by realignment of the complex might more than compensate for the decreased nucleophilicity. Furthermore, it is likely that in the highly heterogeneous environment in the interior of the zeolite the alkene will occupy a variety of different locations. For example, the small amount of hydrogen abstraction from the ethyl group observed in the intrazeolite photooxidations of **2** and **4** could be formed from addition of singlet oxygen to a small amount of alkene found in the supercage void rather than near the zeolite framework (walls).

In support of this new modified Ramamurthy model is the observation that complexation of alkali metal cations to alkenes and aromatic rings are well established in both the gas and condensed phases.²³ In addition, Haw and coworkers²⁴ used solid state NMR to convincingly demonstrate complexation between Li⁺ and benzene in zeolite LiZSM-5. Complexation in our system serves both the function of anchoring the olefin near the wall of the supercage and insuring the proximity of the cation for interaction with the perepoxide as it is formed by the addition of singlet oxygen.

Conclusion

We have provided the first experimental evidence that both cation complexation to the olefin and to the perepoxide are important features of intrazeolite photooxidations. A new model to rationalize these results has been suggested. The orientation of the alkene, the position of the sodium cation,



Scheme 6.

and the direction of approach of singlet oxygen all play important roles in determining the reaction regioselectivity. The interdependence of these factors suggest that in more complex alkenes with alternative binding sites that very different regiochemical outcomes can be expected. Additional studies to provide support for this suggestion are currently in progress and will be reported in due course.

Experimental

Alkenes **1** and **2** were purchased from Aldrich as a mixture. They were separated and purified by preparative gas chromatography on a Gow Mac GC equipped with a thermal conductivity detector and a 30 ft by 3/8 in. column packed with 15% Se-30 on Chromsorb P. Compounds **3–6** and all the allylic hydroperoxides and allylic alcohols have previously been reported and their spectral data were consistent with the literature reports and with their assigned structures.²⁵

Doping of NaY with methylene blue

NaY (Aldrich Lot # 06402LR) was added to distilled water containing MB. The occupancy ($\langle S \rangle = 0.01$ or 0.0001 ; number of MB molecules per supercage) was calculated assuming a composition of the unit cell of $\text{Na}_{56}(\text{AlO}_2)_{56}(\text{SiO}_2)_{136} \cdot 253\text{H}_2\text{O}$ with 8 supercages per unit cell. The mixture was stirred overnight in the dark. The water was decanted and colored zeolite was washed with water and then air dried. The NaMBY was then dried at $100\text{--}120^\circ\text{C}$ for $8\text{--}10$ h at 10^{-4} Torr. It was then removed from the vacuum line and stored in a desiccator prior to use.

Solution photooxidations

CD_3CN solutions 0.05 M in alkenes **1–6**, and 2×10^{-4} M in MB were saturated with oxygen for 15 min and were then irradiated for 30 min with a 600 W tungsten-halogen lamp through 1 cm of a 12 M NaNO_2 filter solution. The reactions were monitored by proton NMR and the product ratios were determined by integration of appropriate peaks. The product ratios are reproducible within $\pm 5\%$.

Intrazeolite photooxidations

A 300 mg sample of NaMBY was added to 5 mL of hexane followed by the addition of sufficient alkene to bring its concentration to between 0.012 and 0.018 M. This mixture was then stirred under a constant stream of oxygen for 15 min followed by irradiation for 10 min through a 550 nm solution cutoff filter. The reactions mixtures were then centrifuged to separate the zeolite. The hexane wet zeolite powder was then placed in a soxhlett cup and extracted for a minimum of 2 h with diethylether. The product ratios were determined by either gas chromatography or by proton NMR. In the gas chromatographic determinations the hydroperoxide mixtures were first reduced by addition of an excess of triphenylphosphine. The resulting diethylether solutions were directly injected onto a HP-1 fused silica column (30 m \times 0.53 mm \times 1.5 μm film thickness) using an injector temperature of 250°C , a flowrate of approximately 1–3 mL/min, and a FID detector

temperature of 300°C . The column temperature was maintained at 40°C for 6 min followed by an increase to 260°C at a rate of $20^\circ\text{C}/\text{min}$ where it was maintained for 15 min. The product ratios were determined using response factors determined from authentic samples of the allylic alcohols. The NMR determinations were made after careful removal of the diethylether immediately following the soxhlett extraction.

Acknowledgements

We thank Professor V. Ramamurthy (Tulane University) for very useful discussions during the course of this study. We also thank the National Science Foundation and the donors of the Petroleum Research Fund, administered by the American Chemical Society, for their generous support of this research.

References

1. For other papers in the series see: (a) Zhou, W.; Clennan, E. L. *J. Am. Chem. Soc.* **1999**, *121*, 2915–2916. (b) Clennan, E. L.; Sram, J. P. *Tetrahedron Lett.* **1999**, *40*, 5275–5278. (c) Zhou, W.; Clennan, E. L. *Chem. Commun.* **1999**, 2261–2262. (d) Zhou, W.; Clennan, E. L. *Org. Lett.* **2000**, *2*, 437–440.
2. Ramamurthy, V.; Eaton, D. F.; Caspar, J. V. *Acc. Chem. Res.* **1992**, *25*, 299–307.
3. Scaiano, J. C.; García, H. *Acc. Chem. Res.* **1999**, *32*, 783–793.
4. Dyer, A. *An Introduction to Zeolite Molecular Sieves*, Wiley: New York, 1988.
5. Derouane, E. G.; Lemos, F.; Naccache, C.; Ribeiro, F. R. *Zeolite Microporous Solids: Synthesis, Structure, and Reactivity*, Kluwer Academic: Dordrecht, The Netherlands, 1992; Vol. 352.
6. Ramamurthy, V.; Sanderson, D. R.; Eaton, D. F. *J. Am. Chem. Soc.* **1993**, *115*, 10438–10439.
7. Tung, C.-H.; Wang, H.; Ying, Y.-M. *J. Am. Chem. Soc.* **1998**, *120*, 5179–5186.
8. Li, X.; Ramamurthy, V. *J. Am. Chem. Soc.* **1996**, *118*, 10666–10667.
9. Robbins, R. J.; Ramamurthy, V. *J. Chem. Soc. Chem. Commun.* **1997**, 1071–1072.
10. Compound **4** was irradiated for 25 min through a 400 nm cutoff filter solution using 1% NaMBY.
11. We thank Professor V. Ramamurthy for making us aware of the decomposition products formed in the intrazeolite photooxidation of 2-methyl-2-heptene.
12. Frimer, A. A.; Stephenson, L. M. In *The Singlet Oxygen Ene Reaction*, Frimer, A. A., Ed.; CRC: Boca Raton, FL, 1985; Vol. II, pp 67–91.
13. Clennan, E. L.; Sram, J. P. *Tetrahedron Lett.* **1999**, *40*, 5275–5278.
14. Rousseau, G.; LePerchec, P.; Conia, J. M. *Tetrahedron Lett.* **1977**, 2517–2520.
15. Lerdal, D.; Foote, C. S. *Tetrahedron Lett.* **1978**, 3227–3230.
16. Orfanopoulos, M.; Grdina, S. M. B.; Stephenson, L. M. *J. Am. Chem. Soc.* **1979**, *101*, 275–276.
17. Schulte-Elte, K. H.; Rautenstrauch, V. *J. Am. Chem. Soc.* **1980**, *102*, 1738–1740.
18. Inagaki, S.; Fujimoto, H.; Fukui, K. *Chem. Lett.* **1976**, 749–752.
19. Stephenson, L. M. *Tetrahedron Lett.* **1980**, *21*, 1005–1008.

20. Houk, K. N.; Williams Jr., J. C.; Mitchell, P. A.; Yamaguchi, K. *J. Am. Chem. Soc.* **1981**, *103*, 949–951.
21. Orfanopoulos, M.; Stratakis, M.; Elemes, Y.; Jensen, F. *J. Am. Chem. Soc.* **1991**, *113*, 3180–3181.
22. Lowry, T. H.; Richardson, K. S. *Mechanism and Theory in Organic Chemistry*, Harper and Row: New York, 1987.
23. Ma, J. C.; Dougherty, D. A. *Chem. Rev.* **1997**, *97*, 1303–1324.
24. Barich, D. H.; Xu, T.; Zhang, J.; Haw, J. F. *Angew. Chem. Int. Ed. Engl.* **1998**, *37*, 2530–2531.
25. Stephenson, L. M.; Grdina, M. J.; Orfanopoulos, M. *Acc. Chem. Res.* **1980**, *13*, 419–425.